Hydration and Dynamics of a Tetramethylammonium Ion in Water: A Computer Simulation Study

L. García-Tarrés and E. Guàrdia*

Departament de Física i Enginyeria Nuclear, Universitat Politècnica de Catalunya, Sor Eulàlia d'Anzizu, Mòdul B4-B5 08034 Barcelona, Spain

Received: March 10, 1998

Molecular dynamics simulations of one single tetramethylammonium ion in water have been carried out. The structural analysis revealed the existence of a well-defined hydration shell. The orientation and dynamics of the hydration shell molecules are analyzed. Residence times and hydration numbers are reported. The dynamical analysis shows that hydration shell water molecules have lower self-diffusion coefficients and higher reorientational times than pure water. Translational and reorientational motions of the ion are studied. The influence of the assumed water model on the different properties is discussed.

Introduction

The hydration of solutes with apolar surfaces in aqueous solutions is a problem of great interest in biological systems. Phenomena such as assembly of micelles and membranes and protein folding are believed to be driven by the interaction between apolar groups.[1−3] Tetramethylammonium (TMA) is a small organic ion that has been used as an ionic model to study hydrophobic behavior in water solutions. Neutron diffraction studies[4,5] and Monte Carlo simulations[6,7] on the TMA ion in water pointed to a weak "apolar" type of hydration. A molecular dynamics simulation of a 0.555 *m* TMACl solution has been recently published,[8] which includes a study of the hydrogen bonding and the high-frequency vibrational motions of hydration shell molecules. In this case, the TMA was treated as a charged "pseudoatom". The aim of the present work is to extend these previous studies and to include an analysis of the dynamical properties of the ion as well as of the hydration shell molecules. A model that explicitly considers the molecular structure of the TMA will be assumed. Similar studies on atomic ions have been previously reported.[9−11] A comparison of the properties of the TMA hydration shell with those of the Na^+ hydration shell molecules will be helpful for understanding hydrophobic effects.

The most important problem to perform realistic simulations is the choice of suitable interaction potentials. In this paper we report the results obtained using simple point charge (SPC and SPC/E) water models.[12,13] Despite their simplicity, they reproduce satisfactorily many properties of liquid water and they are widely used in computer simulations of aqueous solutions. The comparison between the results obtained with the two models will allow us to analyze the sensitivity of the different properties to the assumed water model.

Molecular Dynamics Simulations

Molecular dynamics (MD) simulations were performed on a system containing a single TMA ion and $N = 215$ water molecules in a cubic box with periodic boundary conditions. The side length of the cube was $L = 18.70$ Å which gives a solvent density equal to 1.00 g/cm^3, and the reference temperature was $T_{ref} = 298$ K. The ion and the solvent molecules were modeled by site−site interaction potentials, and the interaction energy between two species was then determined by the sum of the intermolecular interactions between all pairs of sites according to the expression

$$V_{ab} = \sum_{i}^{on\ a} \sum_{j}^{on\ b} \left(\frac{A_i A_j}{r_{ij}^{12}} - \frac{C_i C_j}{r_{ij}^{6}} + \frac{q_i q_j}{r_{ij}} \right) \qquad (1)$$

The coefficients of the short-range part can be expressed in terms of Lennard-Jones parameters, $A_i^2 = 4\epsilon_i\sigma_i^{12}$ and $C_i^2 = 4\epsilon_i\sigma_i^6$, and q_i is the charge assigned to the site. For the TMA ion we adopted the same model as in previous Monte Carlo studies[6,7] where the ion is represented by five sites centered on the nitrogen atom and the carbon atoms of the methyl groups, with $q(CH_3) = 0.25$ e, $d(N-CH_3) = 1.51$ Å, and a tetrahedral geometry. The Lennard-Jones parameters ϵ and σ are listed in Table 1. The SPC[12] and SPC/E[13] are rigid water models with three sites located at the atomic positions. The SPC/E model is a reparametrized version of the SPC model which explicitly includes the water polarization energy[13] with an increase in the molecular dipole moment ($\mu = 2.35$ D for SPC/E, $\mu = 2.27$ D for SPC). The Lennard-Jones parameters and partial charges for both models are collected in Table 1.

To carry out the simulations, we employed the integration algorithm proposed by Berendsen et al.[14] with a time step of 0.002 ps and a thermal bath coupling constant of 0.2 ps. Bond lengths and bond angles where kept fixed by using the SHAKE method.[15] To handle with the long-range Coulombic forces, we used the Ewald summation technique.[16] Each run consisted of an initial equilibration period of 25 ps and a production period of 200 ps. The averaged temperature was 296 K with a deviation less than 2%. Auxiliary simulations of pure water were also carried out. In this case the simulation length was 50 ps.

Structure and Thermodynamics

A. Ion−Water Structure. The ion−water site−site radial distribution functions obtained with the SPC model are shown in Figure 1. Functions corresponding to the SPC/E model have not been plotted since they do not differ significantly from those

S1089-5647(98)01427-8 CCC: $15.00
Published on Web 08/29/1998

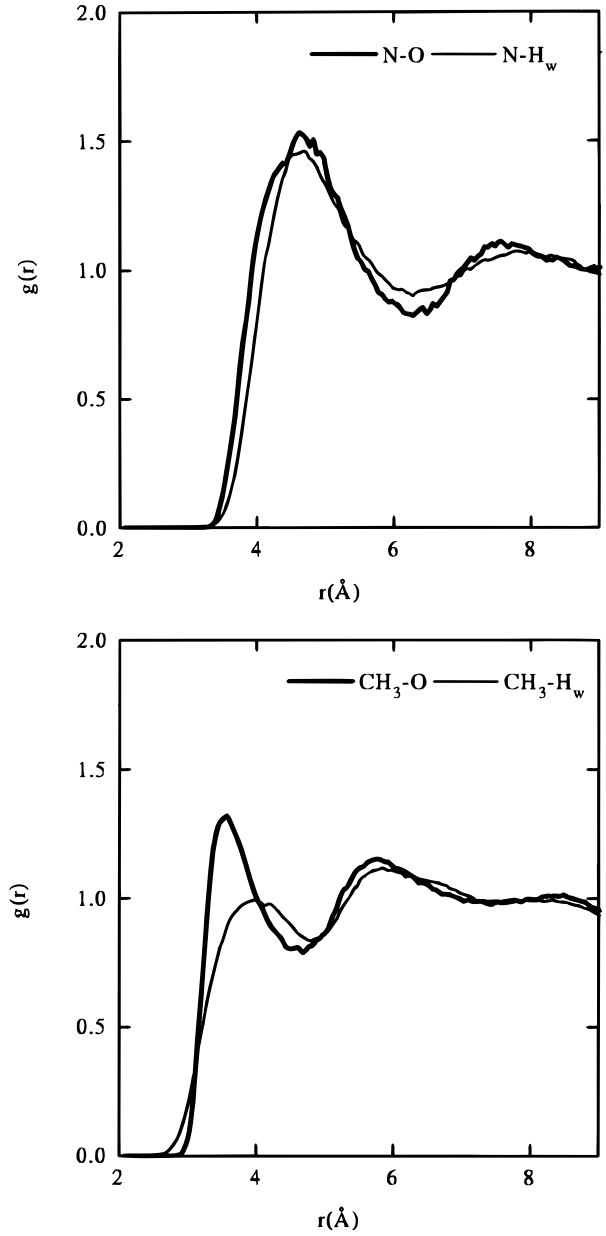

Figure 1. Ion−water radial distribution functions for the SPC model: top: N site; bottom, CH_3 site.

TABLE 1: Parameters for the Interaction Potentials

atom	model	ϵ (kcal/mol)	σ (Å)	q (e)
O	SPC	0.1553	3.166	−0.82
H_w	SPC	0.0	0.0	0.41
O	SPC/E	0.1553	3.166	−0.8476
H_w	SPC/E	0.0	0.0	0.4238
N		0.17	3.25	0.0
CH_3		0.145	3.96	0.25

for SPC. This result is consistent with previous findings for atomic ions.[10,17] Table 2 summarizes the positions of the relevant peaks for the different pairs. The N−H_W and N−O $g(r)$'s show a first peak at the same position, which indicates that hydrogen atoms are, on the average, at the same distance from nitrogen as the oxygens. On the other hand, the oxygen atoms are slightly closer to methyls than the hydrogen atoms (see Figure 1).

As can be seen from Table 2 our ion−water $g(r)$ values are in good agreement with neutron diffraction data[4,5] and with Monte Carlo simulation results.[6] In both cases, the authors

TABLE 2: Ion−Water Radial Distribution Functions Peaks[a]

	SPC model			Jorgensen and Gao[6]			exptl[4]		
$g(r)$	1st max	1st min	2nd max	1st max	1st min	2nd max	1st max	1st min	2nd max
N−H_w	4.65	6.25		4.5					
N−O	4.65	6.25		4.7	5.6				
CH_3−H_w	3.95	4.8	5.85	4.0	4.9	5.9			
CH_3−O	3.55	4.7	5.75	3.5	4.5	5.6			
N−X							4.6	6.3	8

[a] In the case of the experimental data, X refers to a generic solvent atom.

proposed a clathrate cage hydration structure made by water surrounding the ion with both oxygen and hydrogen atoms staying equidistant to TMA nitrogen against the alternative model in which the TMA acts as a cation and the hydration shell molecules are oriented with oxygen toward the ion and hydrogens pointing away.

We also evaluated the running coordination number ($n(r)$)

$$n(r) = 4\pi\rho \int_0^r r'^2\, g(r')\, \mathrm{d}r' \qquad (2)$$

where ρ is the atomic solvent density. The function $n(r)$ gives the mean number of molecules within a sphere of radius r centered on the ion. The coordination number is defined as the plateau value of $n(r)$ at distances close to the first $g(r)$ minimum. By integrating the N−O $g(r)$ up to 6.25 Å, we obtain a coordination number $cn = 30$, while Jorgensen and Gao[6] reported a value of 20. This discrepancy is mainly due to the difference in the position of the N−O $g(r)$ minimum (see Table 2).

To get further insight into the structure of the water molecules around the ion, we computed the mean number densities of oxygen and hydrogen atoms in a plane that contains the N−CH_3 axis. The contour lines for densities differing in the same constant value for both oxygen and hydrogen are shown in Figure 2. Because of the symmetry of the system, only the results for a semiplane have been represented. The plots clearly reflect the tetrahedral geometry of the TMA ion. We can observe the existence of a well-defined quasi-spherical hydration shell. The presence of two peaks for both the oxygen and hydrogen density profiles is also remarkable. One of these two peaks appears along the N−CH_3 axis, on the nitrogen side, and the other can be associated to water molecules close to the CH_3−CH_3 edge.

Orientation of the Water Molecules. The orientation of the water molecules in the hydration shell was analyzed by computing the angle (θ) between the dipole moment of the water molecule and the nitrogen−oxygen position vector. The mean value of cosθ as a function of nitrogen−oxygen distance ($\langle\cos\theta\rangle$) and the probability distribution of cosθ for the hydration shell molecules ($P(\cos\theta)$) obtained with the SPC model are shown in Figure 3. We did not observe any appreciable influence of the water model. The influence of the ion on the orientation of water molecules diminishes as the distance increases, and it is almost negligible beyond the hydration shell. The same qualitative feature was observed for atomic ions.[9] The peak of $P(\cos\theta)$ corresponds to an angle $\theta \approx 116°$. That means that a hydration molecule preferentially orientates with the dipole moment nearly tangent to the sphere centered at the nitrogen atom. This behavior is characteristic of hydrophobic hydration, and it was already observed in computer simulations of methane[18] and ethane[19] in aqueous solution, whereas the molecules of the hydration shell of a Na^+ ion exhibit a trigonal

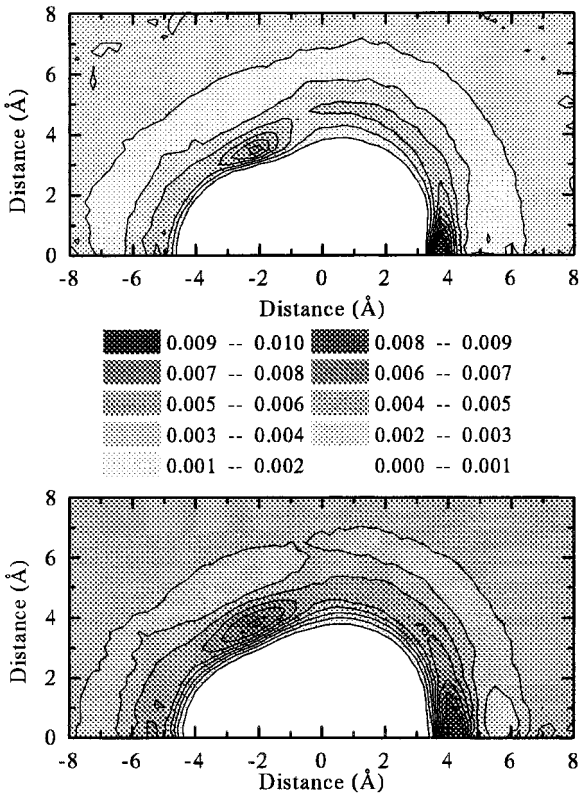

Figure 2. Contour plots of the oxygen (top) and hydrogen (bottom) density profiles around the TMA ion. The horizontal axis corresponds to the N−CH_3 direction.

orientation with θ close to 180°. [9] A snapshot of a configuration with the TMA ion and the hydration shell molecules is shown in Figure 4. We can indeed observe a tangential orientation of the molecules, but with a significant dispersion in the values of θ which in fact is also reflected in the $\langle\cos\theta\rangle$ and $P(\cos\theta)$ functions (see Figure 3).

Enthalpy of Solution. The energy for the process of transferring the solute from the ideal gas phase into the solvent (ΔE_{sol}) can be evaluated from computer simulations as the difference between the total potential energy of the dilute solution (E_S) and the potential energy of the pure solvent (E_W*) . The enthalpy of solution (ΔH_{sol}) can then be given by[20]

$$\Delta H_{sol} = \Delta E_{sol} + P\Delta V_{sol} - RT_{ref} \qquad (3)$$

where (ΔV_{sol}) is the volume of solution ($V - V$*) and the last term is the PV contribution for the solute in the gas phase. The calculated results for ΔH_{sol} and its components are given in Table 3 along with the experimental data.[21,22] The standard deviations of E_S and E_W* are approximately 15 kcal/mol. We can first observe that $\Delta H_{sol} \approx \Delta E_{sol}$ which is a general feature of solutions at normal room conditions. Consistently with a higher molecular dipole moment, both E_S and E_W* are more negative for the SPC/E model than for the SPC model, but the difference $\Delta E_{sol} = E_S - E_W$* has the opposite trend. The resulting ΔH_{sol} with the SPC model is close to the value of −48 kcal/mol reported by Jorgensen and Gao.[6] Both SPC and SPC/E results are compatible with the experimental data which show an important dispersion. Nevertheless, the SPC/E model probably underestimates the enthalpy of solution.

Residence Times and Hydration Numbers

The residence time of water in the hydration shell and the hydration numbers were evaluated by using the procedure

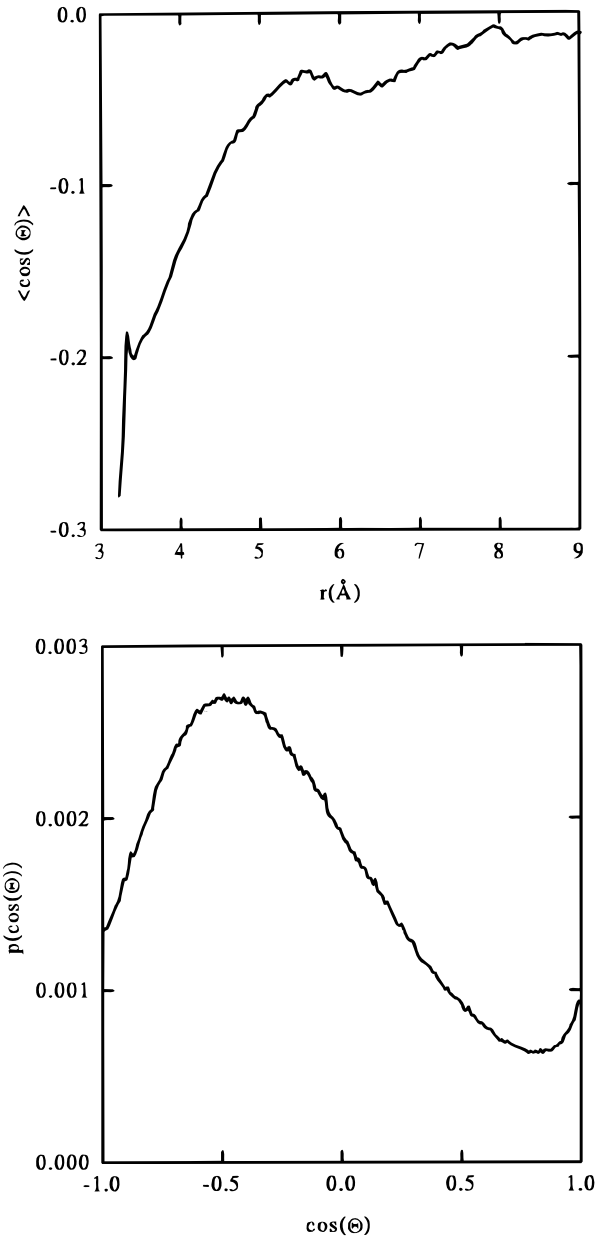

Figure 3. Mean value of cos θ as a function of ion−water distance (top) and probability distribution of cos θ for the hydration shell water (bottom).

described in ref 23. During the simulations we computed the function $n(t)$ which is defined as the number of water molecules that having initially been in the hydration shell remain there after a time t, independently whether they have been outside for any period smaller than t*. Following ref 23, we took t* = 2 ps. We used as the cutoff radius for the hydration shell the position of the first minimum of the N−O $g(r)$, i.e., 6.25 Å (see Table 2). The initial value $n(0)$ is just the coordination number. At long times, the $n(t)$ function shows an exponential decay and the residence time of water in the ion hydration shell (τ_{IW}) is determined by fitting $n(t)$ to the function

$$n(t) = n(0)\exp(-t/\tau_{IW}) \qquad (4)$$

This procedure has been applied to determine the residence time of water molecules around atomic ions,[9,10,17,23] and the values obtained are in reasonable agreement with the ones resulting from a detailed analysis of the hydration shell exchange kinetics.[24] The results for both SPC and SPC/E models are

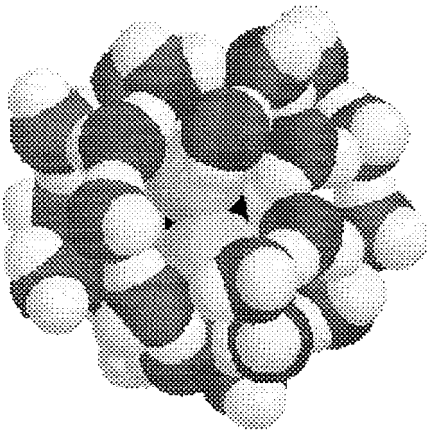

Figure 4. Snapshot of a configuration of the TMA ion (in the middle) and the hydration shell molecules.

TABLE 3: Enthalpy of Solution (kcal/mol)

model	E_S	E_W^*	$P\Delta V_{sol} - RT_{ref}$	ΔH_{sol}	ΔH_{sol} (exptl)
SPC	−2187	−2137	−0.59	−50.0	−41,[a] −53[b]
SPC/E	−2430	−2395	−0.59	−35.0	−41,[a] −53[b]

[a] Reference 21. [b] Reference 22.

TABLE 4: Residence Times (ps) and Hydration Numbers

	SPC model	SPC/E model
$n(0)$	30.4	30.5
τ_{IW}	12.5	18.0
τ_{WW}	3.2	5.5
hn	23.5	22.5

given in Table 4. We observe a greater stability of the hydrate complex for the SPC/E model. The same trend was observed for the Na^+ ion, in which case the reported values were τ_{IW} = 24 ps[9] and τ_{IW} = 29 ps,[17] respectively. It is worthy to note that τ_{IW} is significantly lower for TMA than for Na^+. Finally, we calculated the dynamic hydration number (*hn*), which was defined[23] as the mean number of water molecules that remain within the hydration shell over a period of time in which the first coordination shell in pure water is renewed. The number *hn* is given by

$$hn = cn \exp(-\tau_{WW}/\tau_{IW}) \tag{5}$$

where τ_{WW} is the residence time of a water molecule in the first coordination shell of pure water. The τ_{WW} values were obtained from the pure water simulations by the same procedure used for the determination of τ_{IW}. For those ions for which the residence time is very high, the hydration and coordination numbers are the same. But for intermediate to low τ_{IW} values, *hn* is lower than *cn*, and it is more appropriate to compare with experimental estimates based on experiments involving dynamic processes. An illustrative discussion of this point is given in ref 25. As we can see from Table 4, we obtain for TMA a hydration number of ≃23 which is in good agreement with the value of 25 proposed in ref 26 from NMR experiments on deuterated TMACl solutions.

Dynamics

Translational Motions. To investigate the mobility of the TMA ion and the hydration shell molecules, the self-diffusion coefficients (D) were calculated from the corresponding mean square displacement functions ($r^2(t)$) by following the Einstein relation

$$D = \lim_{t\to\infty} \frac{1}{6t} r^2(t) \tag{6}$$

The $r^2(t)$ functions for both SPC and SPC/E models are shown in Figure 5, and the values are gathered in Table 5. For both water models, the same qualitative results are obtained which are consistent with the findings of NMR experiments on TMABr deuterated solutions.[27] First of all, the self-diffusion coefficient of molecules in the hydration shell is smaller than that for pure water. The same behavior was observed in computer simulation studies of hydrophobic solutes[19,28] and atomic ions.[9,10] In the case of TMA hydration shell, the decrease is approximately 40% and does not depend on the water model. On the other hand, the hydration shell molecules have a higher self-diffusion coefficient than the ion. All D values diminish with the assumption of the SPC/E model and the TMA at infinite dilution,[26] and pure water[29] experimental self-diffusion coefficients are almost reproduced (see Table 5).

To obtain further information on the microscopic dynamics, the normalized atomic velocity autocorrelation functions ($C_V(t)$) were calculated for both TMA and water. The corresponding power spectra ($S_V(\upsilon)$) were then determined by using the expression

$$S_V(\upsilon) = \int_0^\infty C_V(t) \cos(\upsilon t)\, dt \tag{7}$$

Figure 6 shows the functions obtained using the SPC model for the ion and the hydration shell molecules. The results do not differ appreciably when the SPC/E model is used. Both the N and the CH_3 $C_V(t)$ functions show the oscillatory shape characteristic of dense liquids that reflects the oscillations of the ion in the cage formed by the molecules of the hydration shell. Because of these oscillations the N and CH_3 power spectra have a peak at approximately the same position (∼50 cm^{-1}) as the hydration shell oxygen (See Figure 6, bottom). In a computer simulation study of the far-infrared spectra of water,[30] this peak was attributed to the vibrations of water molecules inside the cage formed by their neighbors, while the shoulder centered around 200 cm^{-1} was associated with O−O stretching vibrations of H-bonded molecules. The hydrogen power spectra show a librational band centered at 500 cm^{-1}. Functions corresponding to pure water have not been depicted since they do not differ appreciably from those for the hydration shell. Our findings indicate that the TMA ion does not affect significantly the H-bond network of water. The same conclusion was derived by Hawlicka and Dlugoborski[8] from their analysis of the high-frequency bending and stretching motions of the hydration shell molecules. Slusher and Cummings[31] performed a study of the H-bond network in tetraalkylammonium halide solutions that was based in the analysis of the water−water radial distribution functions, and they concluded that the degree of hydrogen bonding in the hydration shell of TMA is less than that in pure water although the effect is relatively small.

Reorientational Motions. Reorientational motions in liquids are usually studied through a set of time-dependent correlation functions ($C_l(t)$) defined as[32]

$$C_l(t) = \langle P_l(\vec{u}_a(t)\langle\vec{u}_a(0)\rangle \tag{8}$$

were P_l is the lth Legendre polynomial and $\vec{u}_a$ is a unit vector that characterizes the orientation of the molecule. Reorientational correlational times are then calculated by assuming an exponential decay rate of $C_l(t)$ at long times,

$$C_l(t) = \exp(-t/\tau_l) \tag{9}$$

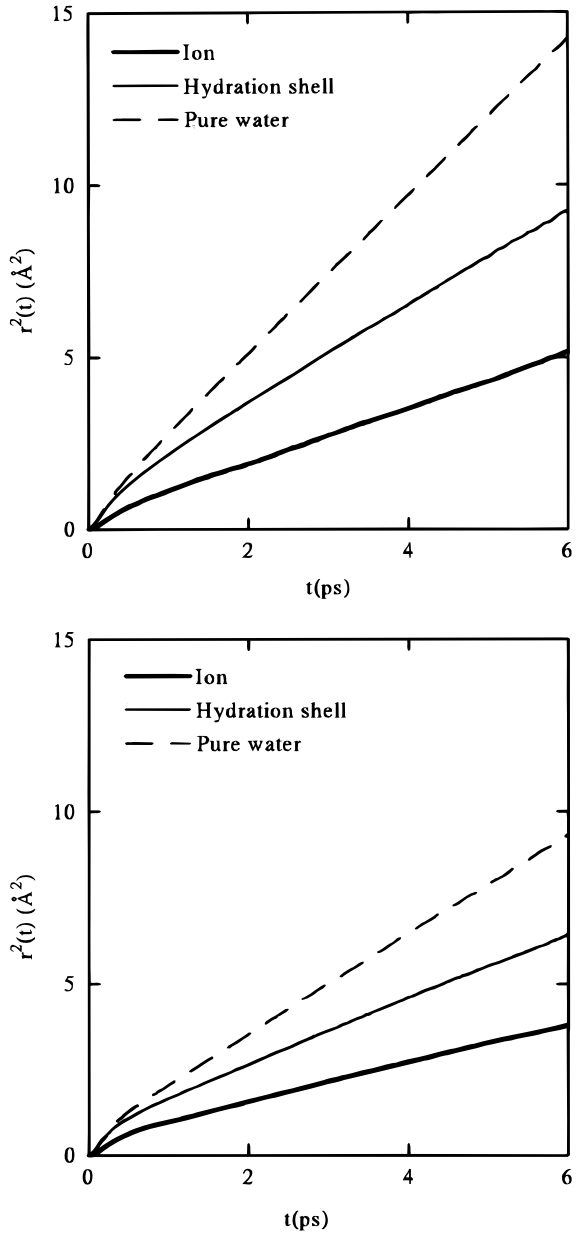

Figure 5. Mean square displacement functions for the TMA ion, hydration shell, and pure water: top, SPC model; bottom, SPC/E model.

TABLE 5: Self-Diffusion Coefficients for the Ion, the Hydration Shell, and Pure Water (D in 10^{-5} cm^2/s)

	SPC model	SPC/E model	exptl
TMA	1.4	0.9	0.93[a]
hydration Shell	2.3	1.5	
pure water	3.7	2.4	2.3[b]

[a] Reference 26 (in deuterated water). [b] Reference 29.

For TMA, two vectors were studied: $\vec{u}_1$ in the N−CH_3 direction and $\vec{u}_2$ in the CH_3−CH_3 direction. For water, three unit vectors were considered: $\vec{u}_1$ in the direction of the dipole moment vector, $\vec{u}_2$ in the intramolecular H_W−H_W direction, and $\vec{u}_3 = \vec{u}_1 \times \vec{u}_2$ orthogonal to the plane of the water molecule. For the study of the reorientation of the ion−water hydrate complex, we also considered the unit vector $\vec{u}_4$ along the N−O direction.

The $C_l(t)$ functions corresponding to the TMA ion and to the hydration shell molecules are shown in Figures 7 and 8, respectively. Tables 6 and 7 summarize the corresponding τ_l values. It is interesting to consider the short time behavior of

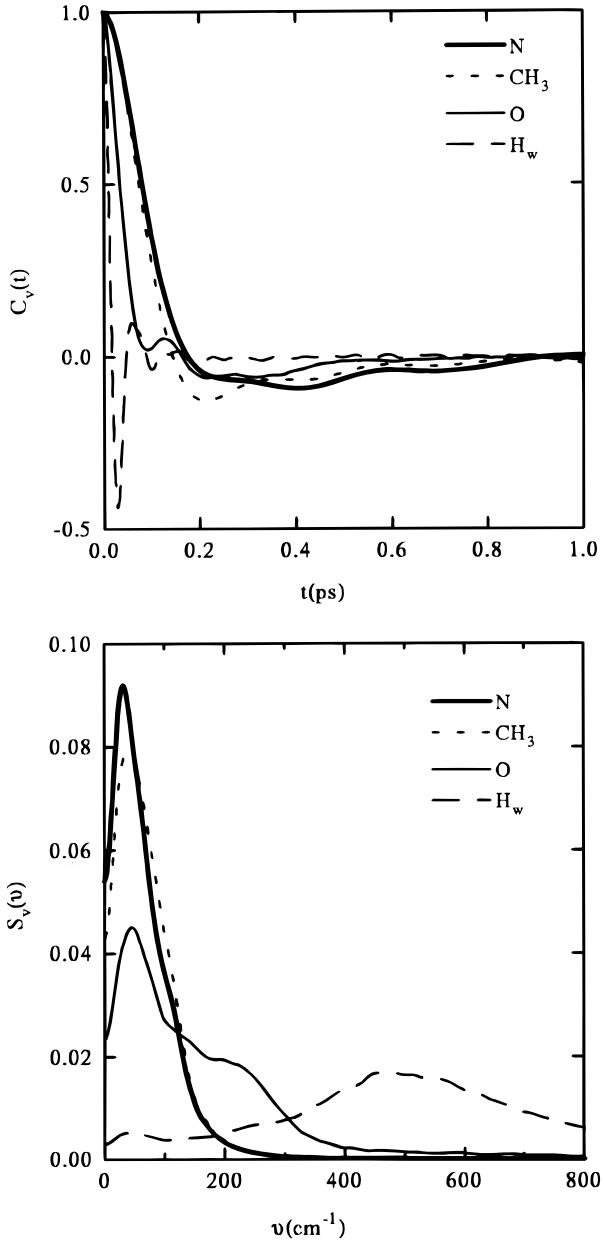

Figure 6. Atomic velocity autocorrelation functions (top) for the TMA ion and hydration shell molecules and their power spectra (bottom).

the functions. For the TMA ion (see Figure 7) we do not see the oscillatory "libration" displayed by the hydration shell $C_l(t)$ functions (see Figure 8) and which is characteristic of H-bonded liquids. The reorientational motion is slightly faster for the N−CH_3 direction than for the CH_3−CH_3 direction. For both directions the ratio τ_1/τ_2 is approximately 2 which indicates a deviation from a purely diffusive rotational motion in which case a ratio $\tau_1/\tau_2 = 3$ should be expected.[32] In the case of the $\vec{u}_4$ vector, this condition is almost fulfilled. The reorientational correlation times of the hydration shell molecules are higher than for pure water, and the ratio is $\tau_{l,\text{shell}}/\tau_1 \approx 1.5$ for all the analyzed directions. This isotropic influence of TMA in water reorientational motions can be attributed to the orientation of the hydration shell molecules. Effectively, the presence of a Na^+ ion influences especially the molecular dipole reorientation with an increment of $\tau_{l,\text{shell}}/\tau_l \approx 3$,[9] whereas for anions, which form linear hydrogen bonds with the hydration shell molecules, the H_W−H_W reorientation is the most affected.[9,10] All values increase with the assumption of the SPC/E model.

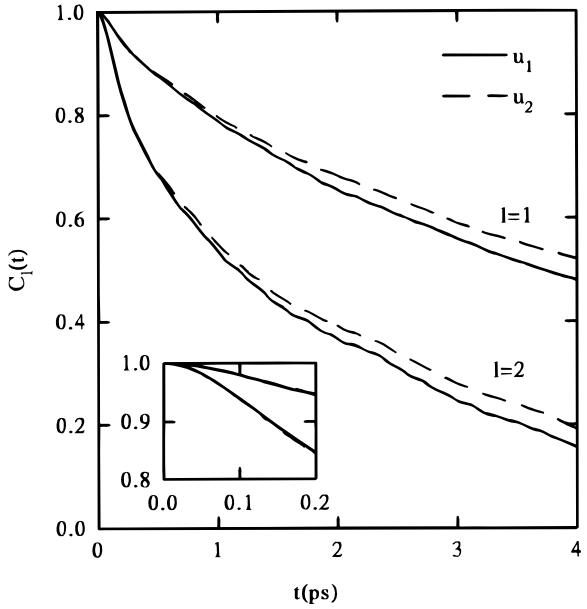

Figure 7. Reorientational time correlation functions of the TMA ion for the SPC model. The insert shows the short-time behavior of the $C_l(t)$ functions.

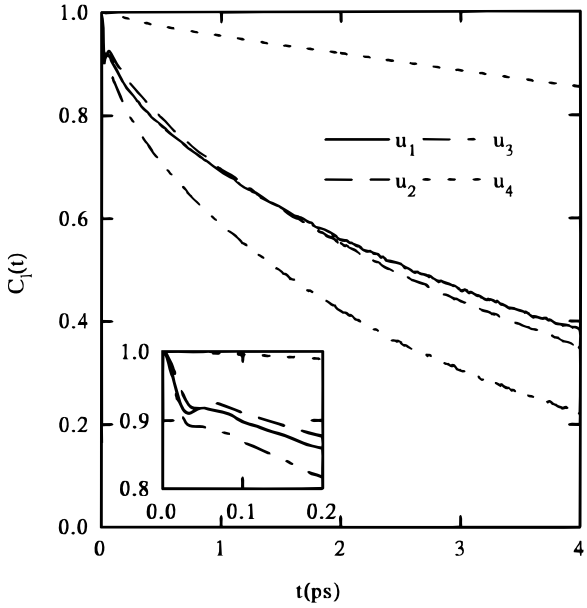

Figure 8. Reorientation time correlation functions of the hydration shell molecules for the SPC model. The insert shows the short-time behavior of the $C_l(t)$ functions.

TABLE 6: TMA Reorientational Correlation Times (τ_l in ps)

vector	l	SPC model	SPC/E model
$\vec{u}_1$	1	5.9	6.9
	2	2.7	4.1
$\vec{u}_2$	1	6.9	7.3
	2	3.1	3.6

Although the comparison of MD results with NMR relaxation data is not straightforward, the TMA reorientational times τ_1 can be reasonably compared with the value $\tau_{+,or} \approx 6$ ps estimated by Bradl et al.[33] for the overall tumbling motion of the cation. As can be seen from Table 6, the τ_1 for the N−CH_3 direction resulting with the SPC model is close to the experimental datum. As far as we know, there is not available experimental information on the TMA hydration shell reorientational times.

TABLE 7: Hydration Shell and Pure Water Reorientational Correlation Times (τ_l in ps)

		hydration shell		pure water	
vector	l	SPC model	SPC/E model	SPC model	SPC/E model
$\vec{u}_1$	1	5.0	7.2	3.1	5.0
	2	2.3	3.2	1.4	2.2
$\vec{u}_2$	1	4.3	7.6	2.8	4.8
	2	2.4	3.8	1.6	2.6
$\vec{u}_3$	1	3.0	5.1	1.9	3.2
	2	1.9	2.8	1.2	1.8
$\vec{u}_4$	1	27.1	40.6		
	2	9.1	13.7		

Some authors tried to relate the reorientational correlation times with the residence time. In the case of pure water, τ_{WW} effectively coincides with the value of τ_1 for the molecular dipole moment direction. But τ_{IW} is markedly higher than any of the hydration shell τ_1 values (see Tables 4 and 7). This suggests that the breakdown of the ion hydration shell involves more complicated mechanisms than a simple molecular reorientation.

Finally, the TMA angular velocity autocorrelation function ($C_\omega(t)$) was also computed. The TMA ion has a symmetric tetrahedral structure, so the center of mass is located at the N atom and all three principal moments of inertia are equal. For such a spherical-top molecule, the angular momentum and the angular velocity are related simply by $\vec{L} = I\vec{\omega}$,, where I is the moment of inertia about a principal axis. The normalized function and its power spectrum ($S_\omega(\upsilon)$) are shown in Figure 9. No significant differences were found between SPC and SPC/E results. The $C_\omega(t)$ function has a oscillatory shape, with a first minimum at 0.2 ps. The function $C_\omega(t)$ obtained by Karim and Haymet[34] for an ammonium ion in water shows a faster initial decay, and the first minimum appears at a shorter time, i.e., $t \approx 0.05$ ps. These differences arise because the ammonium ion is lighter than TMA. The $S_\omega(\upsilon)$ function has a peak at 50 cm^{-1} corresponding to hindering rotations. It is interesting to note that the position of this peak almost coincides with that of the N and CH_3 $S_V(\upsilon)$ (see Figure 6).

The rotational self-diffusion coefficient (D_R) was calculated by using the Green−Kubo relation[34]

$$D_R = \frac{3k_B T_{ref}}{2I} \int_0^\infty \langle \vec{\omega}(t)\vec{\omega}(0)\rangle \, dt \qquad (10)$$

We obtained a value of 0.4×10^{12} rad^2/s. According to our findings on the TMA reorientational times (see Table 6), D_R should be slightly lower for the SPC/E model than for the SPC model. But because of the slow convergence of the integral in eq 10, we could not determine the rotational self-diffusion coefficient with the accuracy required to appreciate these small differences.

Summary

The results of this work corroborate the existence of a well-defined hydration shell around TMA ion. The hydration shell molecules orientate with the dipole moment nearly tangent to the ion, in good agreement with neutron diffraction experiments and previous computer simulations. The hydration shell molecules have lower self-diffusion coefficients and higher reorientational times than pure water. The influence of TMA is the same for all the analyzed molecular reorientations. TMA ions do not influence the low-frequency water power spectra.

The assumption of the SPC or SPC/E water model does not affect the structure nor the short time dynamics. The most

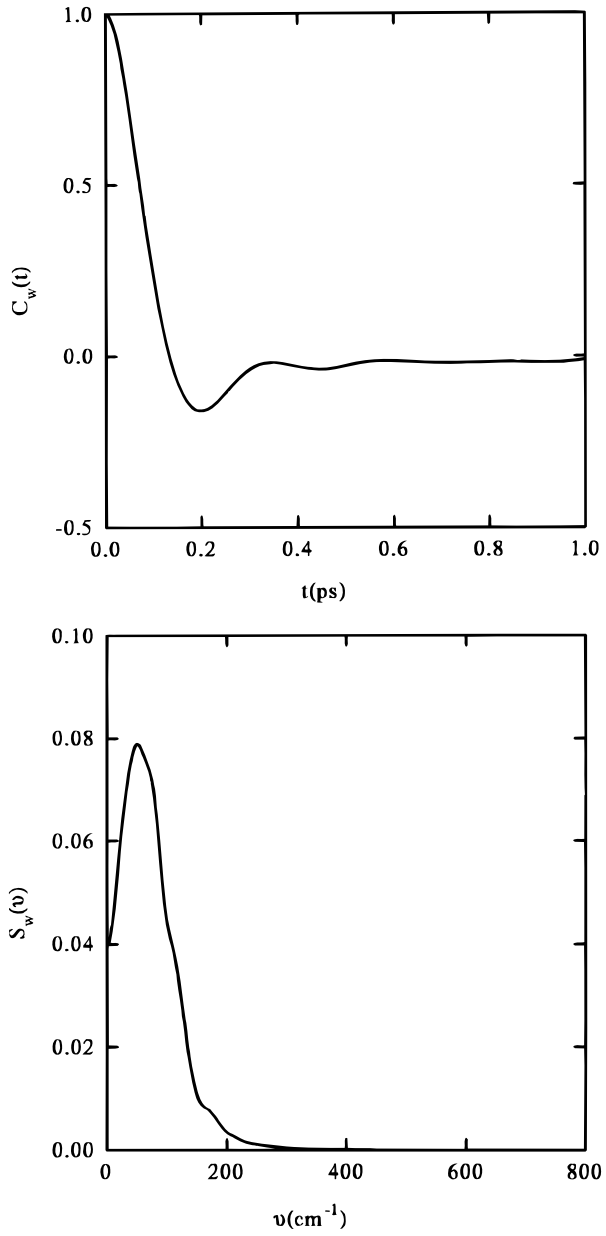

Figure 9. TMA angular velocity autocorrelation function (top) and its power spectrum (bottom) for the SPC model.

significant differences are observed for the enthalpy of solution and the long time dynamics. The self-diffusion coefficients diminish, and the residence time and the reorientational correlation times increase when the SPC/E model is used. The results obtained in this work are in general consistent with the available experimental data. The ΔH_{sol} and the TMA reorientational times are closer to the experiment in the case of the SPC model. The SPC/E model better reproduces the TMA self-diffusion coefficent. We may then conclude that the interaction potentials assumed allow to perform realistic simulations.

Acknowledgment. The simulations reported in this work were carried out at the CEPBA (Centre Europeu de Parallelisme de Barcelona). E.G. gratefully acknowledges the financial support of the Spanish Ministerio de Educación y Cultura (Grants TIC95-0429 and PB96-0170-C03) and the Generalitat de Catalunya (Grant 1995SGR-0618).

References and Notes

(1) *Biophysics of Water*; Franks, F., Ed.; Willey: New York, 1982.
(2) McCammon, J. A.; Harvey, S. C. *Dynamics of Proteins and Nucleic Acids*; Cambridge University Press: Cambridge, 1987.
(3) Robinson, G. W.; Zhu, S. B.; Singh, S.; Evans, M. W. *Water in Biology, Chemistry and Physics*; World Scientific: Singapore, 1996.
(4) Turner, J. Z.; Soper, A. K.; Finney, J. L. *Mol. Phys.* **1990**, *70*, 679.
(5) Turner, J. Z.; Soper, A. K.; Finney, J. L. *J. Chem. Phys.* **1995**, *102*, 5438.
(6) Jorgensen, W. L.; Gao, L. *J. Phys. Chem.* **1986**, *90*, 2174.
(7) Buckner, J. K.; Jorgensen, W. L. *J. Am. Chem. Soc.* **1989**, *111*, 2507.
(8) Hawlicka, E.; Dlugoborski, T. *Chem. Phys. Lett.* **1997**, *268*, 325.
(9) Guàrdia, E.; Padró, J. A. *J. Phys. Chem.* **1990**, *94*, 6049.
(10) Guàrdia, E.; Padró, J. A. *Mol. Simul.* **1996**, *17*, 83.
(11) Guàrdia, E.; Padró, J. A.; Martí, J. In *Femtochemistry, Ultrafast Chemical and Physical Process in Molecular Systems*; Chergui, M., Ed.; World Scientific: Singapore, 1996.
(12) Berendsen, H. J. C.; Postma, J. P. M.; van Gunsteren, W. F.; Hermans, J. In *Intermolecular Forces*; Pullman, B., Ed.; Reidel: Dordrecht, 1981.
(13) Berendsen, H. J. C.; Grigera, J. R.; Straatsma, T. P. *J. Phys. Chem.* **1987**, *91*, 6269.
(14) Berendsen, H. J. C.; Postma, J. P. M.; van Gunsteren, W. F.; di Nola, A.; Haak, J. R. *J. Chem. Phys.* **1984**, *81*, 3684.
(15) Ciccotti, G.; Ferrario, M.; Ryckaert, J. P. *Mol. Phys.* **1982**, *47*, 1253.
(16) Allen, M. P.; Tildesley, D. J. *Computer Simulation of Liquids*; Clarendon: Oxford, 1987; Chapter 5.
(17) Smith, D. E.; Dang, L. X. *J. Chem. Phys.* **1994,** *100*, 3757.
(18) Vaisman, I. I.; Brown, F. K.; Tropsha, A. *J. Phys. Chem.* **1994**, *98*, 5559.
(19) Mancera, R. L.; Buckingham, A. D. *J. Phys. Chem.* **1995**, *99*, 14632.
(20) Chandrasekhar, J.; Jorgensen, W. L. *J. Chem. Phys.* **1982**, *77*, 5080.
(21) Aue, D. H.; Webb, H. M.; Bowers, M. T. *J. Am Chem. Soc.* **1976**, *98*, 318.
(22) Boyd, R. H. *J. Chem. Phys.* **1969,** *51*, 1470.
(23) Impey, R. M.; Madden, P. A.; McDonald, I. R. *J. Phys. Chem.* **1983**, *87*, 5071.
(24) Rey, R.; Hynes, J. T. *J. Phys. Chem.* **1996**, *100*, 5611.
(25) Impey, R. M. In *Molecular-Dynamics Simulation of Statistical-Mechanical Systems*; Giccotti, G., Hoover, W. G., Eds.; North-Holland: Amsterdam, 1986.
(26) Eriksson, P. O.; Lindblom, G.; Burnell, E. E.; Tiddy, G. J. T. *J. Chem. Soc., Faraday Trans. 2* **1988**, *84*, 3129.
(27) Bradl, S.; Lang, E. W. *J. Phys. Chem.* **1993**, *97*, 10463.
(28) Geiger, A.; Rahman, A.; Stillinger, F. H. *J. Chem. Phys.* **1979**, *70*, 263.
(29) Krynichi, K.; Green, C. D.; Sawyer, D. W. *Faraday Discuss., Chem. Soc.* **1979**, *66*, 199.
(30) Martí, J.; Padró, J. A.; Guàrdia, E. *J. Chem. Phys.* **1996**, *105*, 639.
(31) Slusher, J. T.; Cummings, P. T. *J. Phys. Chem. B* **1997**, *101*, 3818.
(32) Hansen, J. P.; McDonald, I. R. *Theory of Simple Liquids*; Academic Press: London, 1986; Chapter 12.
(33) Bradl, S.; Lang, E. W.; Turner, J. Z.; Soper, A. K. *J. Phys. Chem.* **1994**, *98*, 8168.
(34) Karim, O. A.; Haynet, A. D. J. *J. Chem. Phys.* **1990**, *93*, 5961.